Oxidative synthesis and electrochemical studies of poly(aniline-*co*-pyrrole)-hybrid carbon nanostructured composite electrode materials for supercapacitor

Ashok Kumar Sharma[1]*, Preetam Bhardwaj[1], Sundeep Kumar Dhawan[2], Yashpal Sharma[3]

[1]*Department of Materials Science & Nanotechnology, D.C.R. University of Science & Technology, Murthal, India*
[2]*Conducting Polymers Group, National Physical Laboratory, New Delhi, India*
[3]*Post Graduate Department of Chemistry, R.P.S. Degree College, Balana, India*

*Corresponding author. Tel: (+91) 9416337633; E-mail: aksharma210@gmail.com

ABSTRACT

A novel study on conducting polymers based composites involving hybrid carbon nanostructure assemblage of graphene, amine functionalized multiwalled carbon nanotubes and poly(aniline-*co*-pyrrole) has been done. The composites were synthesized by oxidative polymerization of 1:1 mixture of aniline and pyrrole monomer with ammonium per sulphate and ferric chloride oxidants. UV-vis Spectroscopy, Fourier Transform Infrared Spectroscopy (FTIR) and Raman Spectroscopy were used to identify the chemical structure of the obtained composites. Thermal studies indicate that the composites are stable in comparison to poly (aniline-co-pyrrole) alone showing that the hybrid carbon assemblage contributes towards thermal stability in the composites. Crystalline properties of the composites were investigated by X-ray diffraction (XRD). Scanning electron microscopy (SEM) was used to characterize the surface morphology of the composites. The specific capacitance of the composites was characterized by cyclic voltammogram (CV). The capacitive studies reveal that the composite has synergistic effect and highest specific capacitance of 337.35F/g at scan rate of 10mV/sec and 193.06F/g at scan rate of 50 mV/sec was obtained for the composite having thinnest layer of co-polymer over hybrid carbon assemblage i.e., 02-PANI-*co*-PPY-C. Copyright © 2015 VBRI Press.

Keywords: Raman spectroscopy; cyclic voltammetry; scanning electron microscopy; conducting polymers.

Ashok K Sharma got his Ph.D degree in Chemistry in the year 1991 and is currently working as Professor and Chairman in the Department of Materials Science & Nanotechnology, D.C.R University of Science & Technology, Murthal, Sonepat-131039 (Haryana) India. His current research is focused on the development of novel nanomaterials for energy storage and conversion systems.

Sundeep K. Dhawan is working as Chief Scientist at CSIR-National Physical Laboratory, New Delhi – a premier laboratory of CSIR, Ministry of Science & Technology, Govt. of India. He is working in the designing and modification of Conducting polymers, nanoferromagnetic composites, graphene for EMI shielding, organic light emitting diodes & organic solar cells besides developing conducting polymer paints for corrosion protection.

Preetam Bhardwaj did M. Tech. in Materials Science and Nanotechnology in 2012. He is pursuing Ph.D. from Dept. of Materials Science and Nanotechnology, D.C.R University of Science and Technology, Murthal, Sonepat, 131039, Haryana, India under the supervision of Prof. Ashok K. Sharma. Presently he is working in the area of energy storage and EMI Shielding applications of smart Polymers.

Introduction

Supercapacitors have attracted much renewed attention in recent years because of their pulse high power supply, long cycle life (>100,000 cycles), simple operational mechanism, and high dynamics of charge propagation. With the rapid growth of portable electronics, electric vehicles (EV), and hybrid electric vehicles (HEV), there have been increasing demands of high-performance energy storage devices. Supercapacitors, which are also known as electrochemical capacitors or electric double-layer

capacitors, offer a promising alternative to meet the increasing power demand of energy storage systems [1]. Depending on the electrode material and the operational mechanism of supercapacitors, there are three major types of supercapacitors that have attracted intensive activities in research, development, and industrial applications. The first type is using carbon based electrodes and operating without faradaic processes in charging and discharging. For this type of supercapacitors, activated carbon has been the material of choice for nearly forty years since it was first developed for commercial applications in early 1980s [2, 3]. These supercapacitors are based on the mechanism of electrochemical double-layer capacitance. They store the electric charges electrostatically by using reversible adsorption of ions of the electrolyte onto electrodes that are electrochemically stable and have high accessible surface area [4]. Very recently, carbon nanotubes, graphene, and their composites have also been investigated for improving the performance of such supercapacitors [5]. The second type of supercapacitor is oxidation reduction based electrochemical capacitors where transition metal oxides, such as MnO_2 and RuO_2, are utilized for fast and reversible redox reactions to take place at the surface of active materials. The metal oxide usually has a high specific capacitance but often suffers from poor power performance due to its relatively high electrical resistance. The third type of supercapacitors is based on conductive polymers.

Conducting polymers, also called as synthetic metals because of outstanding electrical, electronic and mechanical properties. Various conducting polymers like polyaniline, polyacetylene, polypyrrole and polythiophene have been the subject of intensive research because of their application in different fields ranging from energy storage like supercapacitors to biological like tissue engineering and drug delivery [6, 7]. Among various conducting polymers, polyaniline (PANI) and polypyrrole (PPy) are the most promising materials because of their high electrical conductivity, environmental stability, low cost of production and favorable physiochemical properties [8, 9]. Due to its interesting properties, as explained above, PANI and PPY shows great potential for application in the preparation of chemical sensors, actuators, biosensors and electronic devices and supercapacitors and fuel cells [10, 11]. These conducting polymers can be synthesized chemically as well as electrochemically but chemical method have advantage of mass production and low cost over electrochemical one [12-20]. The conductive polymers offer a high specific capacitance and low production cost, though the conductive polymer based supercapacitors usually have poor stability during cycling because of the destabilization of the polymeric backbone structure.

Graphene and Carbon nanotubes have attracted much interest due to their unusual two and one dimensional structure with novel properties. With potential applications ranging from energy storage devices, molecular electronics and field-emission displays to nanocomposites, graphene and carbon nanotubes (CNTs) offer tremendous opportunity in the development of multi-functional material systems. Exceedingly high electronic properties of the graphene and carbon nanotubes have attracted attention for the development of super conducting light weight structures. Carbon nanotubes (CNTs), after its discovery in 1991, have become one of the most interesting and promising materials [21]. Various investigations have been carried out to discover the potential applications of CNTs, such as hydrogen storage, electron field emission sources, light emitting diodes, electronic devices and biomaterials applications such as tissue engineering scaffolds and drug delivery because of its unique properties such as large specific surface area, high electron transfer rate, high electrocatalytic activity and low electrode fouling. On the other hand graphene is a 2D single layer of carbon atoms with the hexagonal packed structure [22]. Because of its properties like chemical, thermal and mechanical stability, high conductivity and high specific surface area, graphene can be used for numerous applications in the field of energy storage and devices, bio medicals etc. CNT and their derivatives are important filler materials for polymer composites. The properties and performances of graphene–polymer composites not only depend on the quality of graphene filler and polymer matrix, but also depend on the dispersity of the filler, the bonding between the filler and matrix, and the ratio of filler to matrix. These factors are mainly determined by the fabrication processes. Similar to the conventional polymer processing, the methods applied for the fabrication of CNT/graphene–polymer composites are solution mixing, melt blending and oxidative polymerization. Out of these methods in-situ polymerization method is best one to fabricate polymer composites for bulk synthesis. On account of various tremendous properties of conducting polymers, CNTs and graphene, it is reasonable to develop a nanostructured hybrid composite so that the properties of the materials can be enhanced and the composite can be used for advanced applications like charge storage and conversion.

In this study we focused on the synthesis of composite electrode materials with optimized thickness of Co-polymer films prepared on carbon substrate, their morphological, structural, physicochemical and electrochemical properties and possible use as supercapacitor electrode material.

Experimental

Material

Aniline (99 %), pyrrole (98 %), ammonium per sulphate (APS, $(NH_4)_2S_2O_8$, 98 %), and ferric chloride ($FeCl_3$), were purchased from Sigma Aldrich, Germany. Amine functionalized multiwalled carbon nanotubes (Nanocyl, Belgium) and graphene (XG Science, USA) were used as such without any purification. All other chemicals like hydrochloric acid, methanol, sulphuric acid, N,N-dimethylformamide (DMF), PVDF (Sigma Aldrich) were used as received and all were of analytical grade. Solutions were prepared in deionized water. Aniline and pyrrole was vacuum distilled before use.

Method

Monomers, aniline and pyrrole were purified by vaccum-distillation. Equal amounts (0.1g) of amine functionalized MWCNTs and graphene were ultrasonicated for 2 hours in 20% aqueous methanol prior to polymerization. 20% aqueous methanol was found to be the optimum for uniform dispersion of graphene and amine functionalized multiwalled carbon nanotubes. The monomers solution of

aniline and pyrrole in different concentrations (0.02, 0.05, 0.1, 0.2M) was added to hybrid carbon assemblage solution separately. The molar ratios of Aniline and Pyrrole monomers were kept 1:1. 0.5M oxidant solutions of ammonium per sulphate (APS) and ferric chloride (FeCl₃) were added drop wise to the filler and matrix phase solutions i.e. hybrid carbon assemblage and monomer solution at low temperature to control the rate of polymerization. The mixture was left for polymerization for 5 hrs at about 0-5 °C temperature with constant stirring. Basically, there are four parameters that affect the course of the reaction and the nature of final product, that are 1) nature of the synthesis medium, 2) concentration of the oxidant, 3) duration of the reaction, and 4) temperature of the synthesis medium [23]. All these parameters were controlled during the course of reaction. The greenish-black colored powder of Poly(aniline-co-pyrrole)-hybrid carbon assemblage composites were obtained by filtering and rinsing the reaction mixture with deionized water and methanol followed by drying of the remaining powder under vacuum at 60°C for 24h. Methanol washing is desirable to remove the oligomeric and unreacted impurities.

Preparation of electrodes

The poly(aniline-co-pyrrole)-hybrid carbon assemblage based composites were mixed with 15wt % of activated carbon as conductor and 5wt% of binder (PVDF) in N,N-Dimethyl formamide (DMF) solvent. The mixture was ultrasonicated for 1hr and then stirred at ambient temperature to form uniform slurry. The electrodes were fabricated by coating the slurry on 2×2cm² of graphite sheet current collector. The prepared electrodes were dried in vacuum at 60°C for 24h. Remaining electrodes of various composites, poly(aniline-co-pyrrole) and hybrid carbon assemblage were prepared using similar procedure.

Characterization

Infrared spectrum (KBr pellet) was recorded by using Fourier transform infrared spectrophotometer (Perkin Elmer spectrum BXII FTIR) to identify the chemical structure of the prepared composites. The infrared spectrum of the samples utilized in this study was compared with that reported in the literature. The scanning electron microscopy (SEM, JEOL-JSM-5600LV @ accelerating voltage 20kv) was used to examine the surface morphology of Poly(aniline-co-pyrrole)-hybrid carbon assemblage composites. The ordered structures of composites were studied by XRD. X-ray diffraction data was obtained on a Philips (Xpert PRO) machine using CuKα source and fitted with an X'celerator detector (PW 3050/60). Data were collected at 2θ with varying intensity. The diffractogram was in terms of 2θ in the range 5–80°. Renishaw Raman spectrometer is used for Raman analysis. Thermal studies were done using Perkin-Elmer TGA Instrument. The composite electrodes were tested in a beaker type three electrode cell with a reference electrode (Ag/AgCl) and a counter electrode (Pt) by means of potentiostat/galvanostat (CH-Autolab Instruments, 600C series). The electrolyte used was 2M NaPTS + 0.1M p-toluene sulphonic acid solutions; a buffer solution of pH4 and the geometric

surface area of the working electrode was 2×2 cm². An insight into the thermal stability and electronic structure of the composites is also obtained by using TGA and spectral studies respectively. The electrochemical behavior of the co-polymer and the composite materials has been evaluated electrochemically.

Results and discussion

FTIR spectra

FTIR spectra of poly(aniline-co-pyrrole) and poly(aniline-co-pyrrole)-hybrid carbon assemblage composite is represented as **Fig. 1(a and b)**.
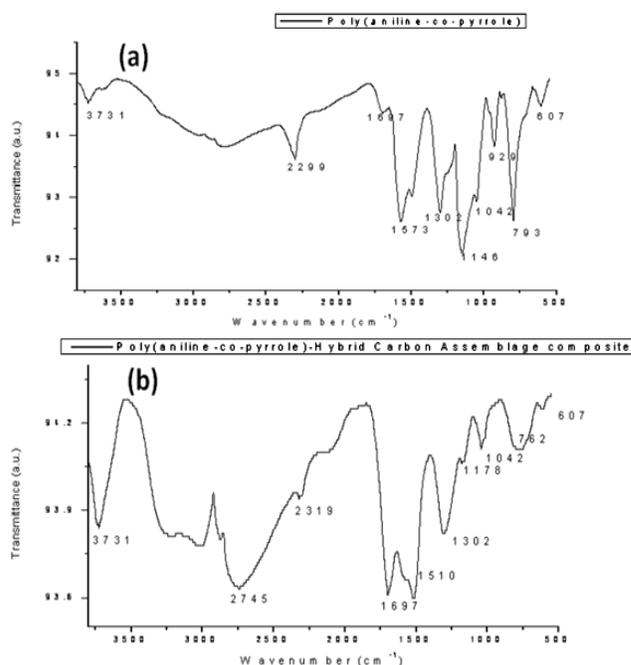
Fig. 1. (a) FTIR spectra of poly(aniline-*co*-pyrrole) and (b) FTIR spectra of poly(aniline-co-pyrrole)-hybrid carbon assemblage composite.

The composite shows all the bands for PANI, PPY, amine functionalized CNT and graphene. It confirms the formation of the copolymer over the hybrid carbon assemblage surface. For polypyrrole, the bands at 793 and 1042cm⁻¹ correspond to C-H out of plane and C-H in plane deformation vibrations respectively. The C-N stretching vibrations of the PPY ring can be seen at 1302cm⁻¹. The strong bands in the region 900-1800 cm⁻¹ indicates that the conductive form of PPy is formed [24, 25]. The C=C of hybrid carbon assemblage shown at 1697cm⁻¹. For polyaniline, the peaks at 1573cm⁻¹ and 1457cm⁻¹ are attributed to quinoid and benzenoid ring stretching vibrations respectively [5, 10, 23-25]. The spectrum assigned N-H vibrations at 3731cm⁻¹ in both copolymer and the assemblage composite. It is observed that the bands shifted to a lower wavenumber for the copolymer (poly (aniline-co-pyrrole)) demonstrating the presence of neighboring aniline and pyrrole constitutional units as compared to composite spectrum. The band at 1146cm⁻¹ is due to conducting form of polyaniline, the emeraldine salt [11, 24]. The bands obtained at 607cm⁻¹, 762cm⁻¹, 1042cm⁻¹, 1178cm⁻¹, 1302cm⁻¹, 1573cm⁻¹ and 1457cm⁻¹ ensures the

formation of poly(aniline-co-pyrrole) over hybrid carbon assemblage. Further two more bands at 2299 and 2319 cm^{-1} represent aliphatic amines. All the common bands were visible in the spectrum and also indicated that there was shifting of peaks after deposition of copolymer over hybrid carbon assemblage. The present FTIR spectra are in agreement with theoretical prediction.

Raman spectra

Fig. 2 is the Raman spectra of poly(aniline-co-pyrrole), hybrid carbon assemblage and composite. The prominent peaks that emerged in the spectrum of poly(aniline-co-pyrrole) can also be observed in the spectrum of Poly(aniline-co-pyrrole)-hybrid carbon assemblage composite. The peak at 850cm^{-1} has been assigned for in-plane ring deformation of quinoid ring and the peak at 883cm^{-1} is due to in-plane benzenoid ring deformation of polyaniline (PANI). The peaks at 937 cm^{-1} and 1047 cm^{-1} have been associated with the quinonoid bipolaron structure and quinonoid polaron structure of polypyrrole [23, 27-29].
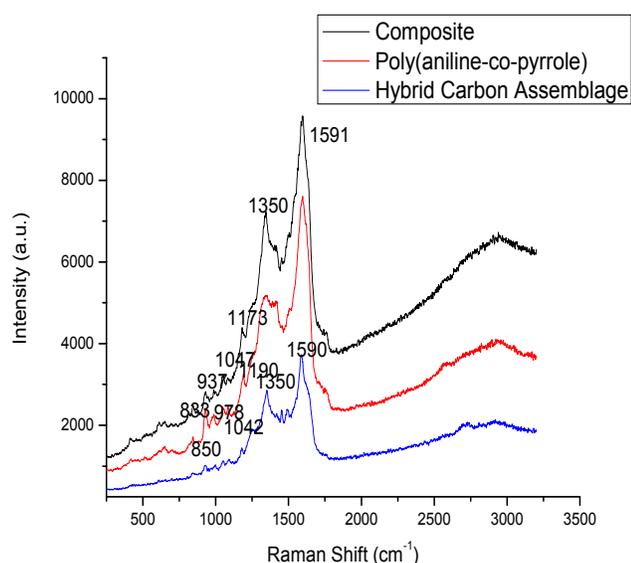
Fig. 2. Raman spectra of poly(aniline-co-pyrrole), hybrid carbon assemblage and poly(aniline-co-pyrrole)-hybrid carbon assemblage composite.

The peak at 1173cm^{-1} is assigned to C-H in plane bending vibration of quinoid ring state. The peak at 1190cm^{-1} has been assigned to C-H in plane bending of benzene ring state. The peaks at 1350 cm^{-1} and 1591 cm^{-1} in the spectrums were assigned to the C-N^{+} stretching vibration of the semiquinone radical state and C-C ring stretching vibration of quinoid ring state [23, 27-31]. Corresponding to C=N stretching vibration in quinoid ring, the peak is shown at 1457cm^{-1} [30]. Raman spectrum of hybrid carbon assemblage describes the structural changes in graphite materials. The spectrum of hybrid carbon assemblage displays two obvious peaks: the well known D band around 1350 cm^{-1}, which is a double-resonance Raman mode, is usually understood as a measurement of structural disorder coming from amorphous carbon and any defects; and the G-band around 1590 cm^{-1}, which is associated to the tangential-mode peaks. G band is

generated by sp^{2} carbons while D band exists because of vibration of sp^{3} carbons or some disordered carbon structure. It has been concluded that when polymer chains are grafted to the surface of hybrid carbon assemblage via covalent bond, the original sp^{2} carbons are converted to sp^{3} carbons, and therefore the relative of sp^{3}/sp^{2} peak intensity ratio should increase [31] as manifested in the spectrum.

UV-visible spectra

The UV-Visible spectra of Hybrid carbon assemblage, Poly(aniline-co-pyrrole) and Poly(aniline-co-pyrrole)-hybrid carbon assemblage composite is illustrated in **Fig. 3**. The UV-Visible spectra were recorded in ethanol. The hybrid carbon assemblage has no characteristic peak in the region 300-800nm. It shows a small broadened peak at 205nm. The Poly(aniline-co-pyrrole) absorption spectra shows characteristic peaks at 210nm, 265nm and 385nm. Similar characteristics peaks were observed in the UV-Visible spectrum of the composite. When aniline is copolymerized with pyrrole and copolymer film is formed over the hybrid carbon assemblage composite, the absorption peaks were shifted to higher wavelengths. This may be due to some interaction of conjugated copolymers with the carbon material. The bands above 380-400nm were due to the polaron to conduction band of PANI and the band over 455nm corresponds to the bipolaron band of polypyrrole [24, 25]. The existence of band at ~380nm in both UV-visible spectra (composite and Poly(aniline-co-pyrrole)) ensured the emeraldine structure of PANI [23-25].
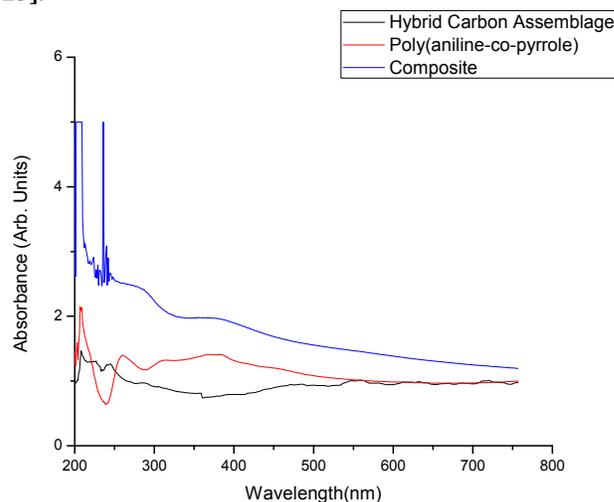
Fig. 3. UV-vis spectra of poly(aniline-co-pyrrole), hybrid carbon assemblage and poly(aniline-co-pyrrole)-hybrid carbon assemblage composite.

X-ray diffraction

X-ray diffraction data of the composites and copolymer is shown in **Fig. 4**. In poly(aniline-co-pyrrole) sample, the peak at 2θ=15° and 25°indicate the presence of aniline and pyrrole. The XRD pattern clearly shows the amorphous behavior of poly(aniline-co-pyrrole) sample that is indicated by the broadness of XRD peak. Whereas, the XRD pattern of poly(aniline-co-pyrrole)-hybrid carbon assemblage composite shows highly crystalline nature of composite due to the incorporation of AMWCNTs and graphene into poly(aniline-co-pyrrole). The peaks at

$2\theta=26°$, $43°$ and $54°$ correspond to the graphitic peaks of AMWCNTs and graphene. PANI gives a sharp peak at around $2\theta = 25°$. Additionally peaks were also observed at $15°$ and $20°$. This indicates that the PANI films are highly crystalline [5, 10, 24, 25, 31]. The peak at $20°$ and $25°$ can be ascribed to the periodicity parallel and perpendicular to the polymer chains of PANI respectively. The peak at 2θ $=15°$ suggests the significant crystallization upon protonation. The broader peaks observed around $25°$ for PANI-PPy copolymer is characteristic of amorphous PPy, as well as the scattering of PPy chains at the interplanar spacing [24-26]. The absence of peaks at $2\theta=44°$ and $54°$ in the XRD of poly(aniline-co-pyrrole) proves the absence of AMWCNTs and graphene.
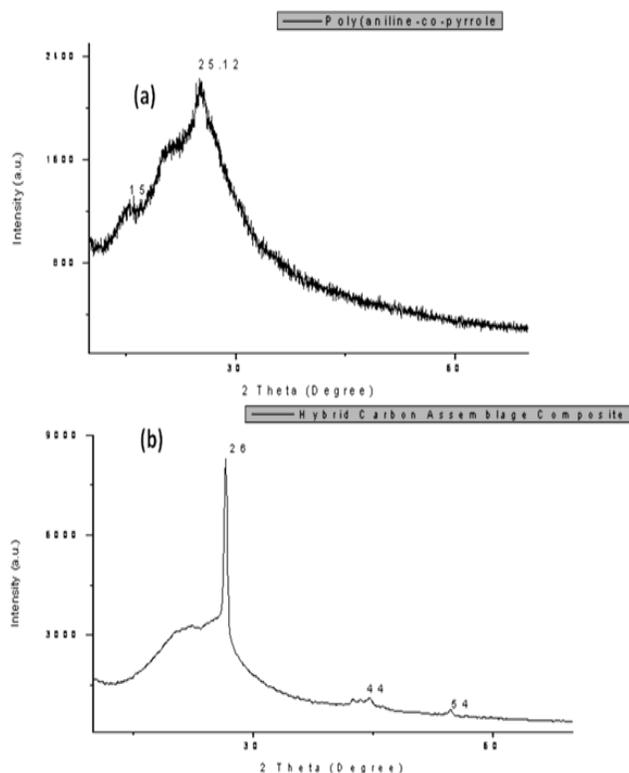
Fig. 4. XRD pattern of (a) poly(aniline-co-pyrrole) and (b) poly(aniline-co-pyrrole)-hybrid carbon assemblage composite.

TGA studies

The thermal analysis of the hybrid carbon assemblage, PANI-co-PPY and the composites was done by heating the material under nitrogen atmosphere with a purge rate of 10mL/min and the analysis between % mass losses with respect to temperature had been done. The thermal analysis of the materials is depicted in **Fig. 5**. The heating rate was kept at 10°C/min and test was done from room temperature to 750°C. From the TGA graph it can be inferred that the hybrid carbon assemblage has highest thermal stability. The copolymer has lowest thermal stability and shows a regular weight loss on uniform heating [25]. At temperature range of 550-630°C the copolymer lost around 75-80% of its weight. The early weight loss of 10-15% at temperature range of 100-120°C is due to presence of some water content in the polymer. The composite has higher thermal stability than the copolymer but lower than the hybrid carbon assemblage. The higher thermal stability of the

composites can be attributed to the presence of hybrid carbon assemblage in to the polymer backbone. Among the composites synthesized, highest thermal stability was shown by 02PANI-co-PPY-C composite because of presence of lower monomer content and formation of thinnest polymeric film that leads to better adhesion between substrate and grown polymeric film.
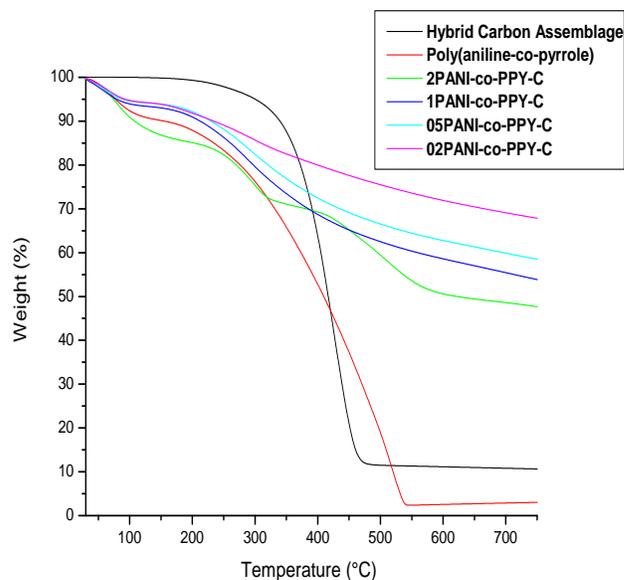
Fig. 5. TGA plot of hybrid carbon assemblage, poly(aniline-co-pyrrole) and composites at the range of 30-750 °C.
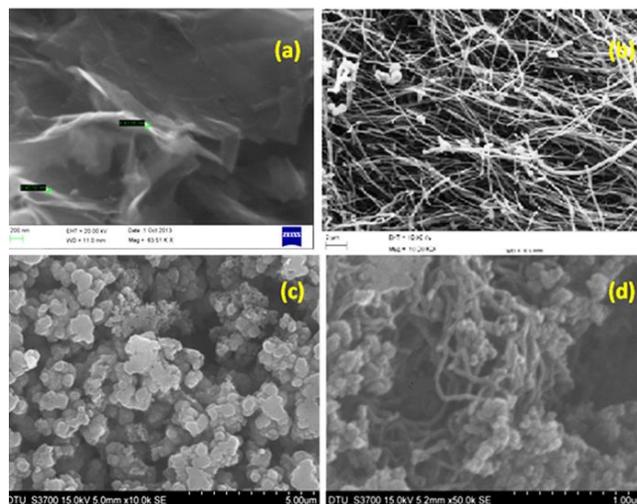
Fig. 6. SEM micrographs of (a) graphene (b) AMWCNTs, (c) Poly(aniline-co-pyrrole) and (d) poly(aniline-co-pyrrole)-hybrid carbon assemblage composite.

Surface morphology

SEM micrographs of the graphene and amine functionalized multiwalled carbon nanotubes are shown in **Fig. 6 (a and b)** while **Fig. 6 (c and d)** represent SEM micrographs of poly(aniline-co-pyrrole) and hybrid carbon assemblage composite. It is observed that graphene is two dimensional sheets of carbon atoms and AMWCNTs are hollow cylindrical shaped tubes structure of carbon atoms of poly(aniline-co-pyrrole) and hybrid carbon assemblage composite. It is able to say that the pyrrole and aniline

monomer in the feed affected the morphology of the obtained copolymer. The copolymer obtained has more irregular, disordered amorphous structures of spherical agglomerates as in **Fig. 6**. It is known that the π-π* interactions between the pyrrole main chain are quite strong and that is why it had a tendency to aggregate into the irregular morphology **[24]**. It is also predicted that the morphology of polypyrrole is dependent on the reaction time **[24, 25]**. By introducing AMWCNTS and graphene in copolymer, the amorphous behavior is reduced and leading to a highly crystalline composite structure as shown in XRD pattern and SEM micrograph **[31, 32]**. SEM micrographs clearly reveal the deposition of copolymer layer over carbon assemblage.
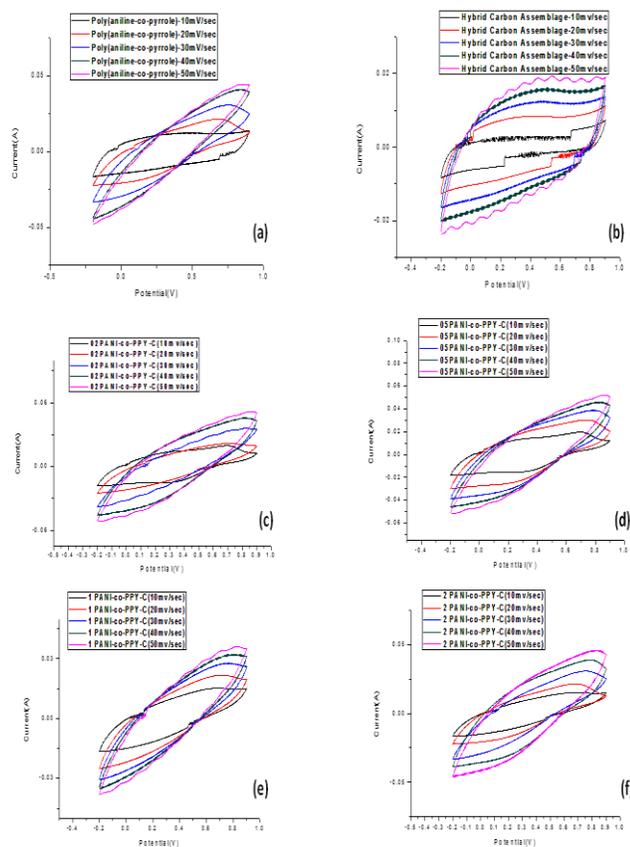
Fig. 7. CV plot of (a) poly(aniline-co-pyrrole) (b) hybrid carbon assemblage (c) 02-PANI-CO-PPY-C (0.02M Copolymers content) (d) 05-PANI-CO-PPY-C (0.05M copolymers content) (e) 1-PANI-CO-PPY-C (0.1M copolymers content) and (f) 2-PANI-CO-PPY-C (0.2M copolymers content).

Cyclic voltammetric studies

Cyclic Voltammetric (CV) measurements for half-cells made of hybrid carbon assemblage, poly(aniline-co-pyrrole) and different poly(aniline-co-pyrrole)-hybrid carbon assemblage composites were carried out in a potential range of -0.2-0.9V (potential window) at scan rates of 10 to 50mV/Sec in 2M NaPTS+0.1M p-toluene sulphonic acid, a buffer solution of pH-4 to examine the electrochemical characteristics. The capacitance value of each sample was calculated from cyclic voltammograms by the following relationship.

Capacitance = Average current/ Scan rate

The specific capacitance value for each sample was calculated by the following relation:

Sp. capacitance = Capacitance/ Weight of electrode

Fig. 7 (a) represents cyclic voltammogram of Poly(aniline-co-pyrrole) that reported a specific capacitance of 107.04F/g at 10 mV/sec. At 50mV/sec reported value is 46.43F/g, this shows that it retains nearly 45% value at 5 times more scan rate. The Voltammogram of hybrid carbon assemblage is given in **Fig. 7 (b)** which show a specific capacitance of 37.66 F/g and 20.86 F/g at scan rates of 10mV/sec and 50mV/sec respectively, indicating that the hybrid carbon assemblage is having high electron conductivity and is a good substrate for deposition of Poly(aniline-co-pyrrole) layer. **Fig. 7 (c-f)** represents the pseudo-capacitive behavior of composites of different composition. The anodic and cathodic peaks for lowest molar content of monomers composite i.e. 02PANI-CO-PPY-C increased consistently indicating that this composite is highly reversible and can be useful at higher scan rates. Variation of specific capacitance of pure poly(aniline-co-pyrrole), hybrid carbon assemblage and different composites at various scan rates were plotted as in **Fig. 8**.
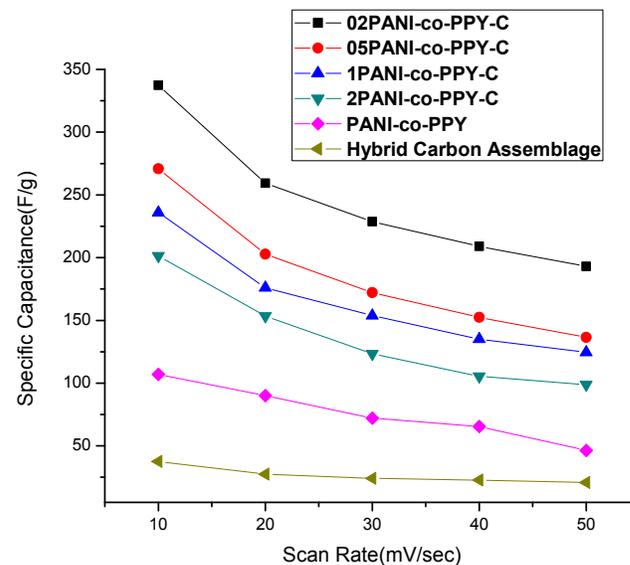
Fig. 8. Plot between scan rate and specific capacitance.

From the plot it is able to conclude that 02PANI-co-PPY-C had highest specific capacitance value of 337.35F/g at scan rate of 10mV/sec and 193.06F/g at 50mV/sec. The % loss of specific capacitance is only 25% as scan rate increases 5 times; therefore the composite material was stable at high scan rates also. From **Fig. 8** we are able to say that specific capacitance of the carbon assemblage alone is not so high but rectangular shape of CV inferred that it can be used as good filler in the polymer matrix to improve the conductance of the materials. In case of composites lowest specific capacitance was obtained from 2PANI-co-PPY-C which has thickest layer of the copolymer deposited over carbon assemblage while highest specific capacitance was obtained with 02PANI-co-PPY-C

composite having thinnest layer of copolymer. This is because of the reason that in case of the thicker conducting polymer layers, a penetration depth of ions is not fully developed as much as the layer thickness so that some portions of the conducting polymer masses are not worked as an active mass while in case of thinnest layer contact resistance among the conducting polymer-hybrid carbon assemblage strips and between current collector surfaces is lowest. So due to combined effect of lower contact resistance and better electrolyte access the composite having thinnest layer of copolymer over carbon assemblage showed highest specific capacitance [11, 13, 19].

Conclusion

Composites of poly(aniline-co-pyrrole)-hybrid carbon assemblage have been prepared successfully. Incorporation of AMWCNTS and graphene in copolymer leads to reduced amorphous behavior and enhanced crystallinity in composite material as exhibited in XRD pattern and SEM micrographs. The composites had higher thermal stability than the copolymer. Cyclic voltammograms of the thinnest layer of co-polymer over carbon assemblage i.e. 02-PANI-CO-PPY-C composite exhibited highest capacitance of 337.35F/g at 10mv/sec scan rate and 193.06F/g at 50mV/sec. supports the fact that the composite material is reasonably stable even at higher scan rates and is proposed as a promising electrode material for future electrochemical supercapacitor applications.

Reference

1. Conway, B.E.; Pell, W.; in Proceedings of the Eighth International Seminar on Double-layer Capacitors and Similar Energy Storage Devices, Florida Educational Seminars, Deerfield Beach, FL, 7–9 December **1998**.
2. Conway, B.E; Electrochemical Capacitors, Kluwer Academic/Plenum Publishers, New York, **1999**.
3. Ryu, K.S.; Kim, K.M.; Park, N.G.; Park, Y.J.; Chang, S.H.; *J. Power Sources* **2002**, *103*, 305.
    DOI: 10.1016/S0378-7753(01)00862-X
4. Cheng, Q.; Tang, J.; Ma, J.; Zhang, H.; Shinya, N.; Qin, L.-C.; *Phys. Chem. Chem. Phys.* **2011**, *13*, 17615.
    DOI: 10.1039/C1CP21910C
5. Sharma, A.K.; Sharma, Y.; Malhotra, R.; Sharma, J.K.; *Adv. Mat. Lett.* **2012**, *3(2)*, 82.
    DOI: 10.5185/amlett.2012.1315
6. Sharma, A.K.; Sharma, Y.; *J. Electrochem. Sci. Eng.* **2013**, *3(2)*, 47.
    DOI: 10.5599/jese.2013.0029
7. Frackowiak, E.; Khomenko, V.; Jurewicz, K.; Lota, K.; Beguin, F.; *J. Power Sources* **2006**, *153*, 413.
    DOI: 10.1016/j.jpowsour.2005.05.030
8. Schultze, J.W.; Karabulut, H.; *Electrochim. Acta* **2005**, *50,* 1739.
    DOI: 10.1016/j.electacta.2004.10.023
9. Arbizzani, C.; Mastragostino, M.; Scosati, B.; in Nalwa, H.S.; (Ed.), Handbook of Organic Conductive Molecules and Polymers, vol. 4, Wiley, Chichester, UK, **1997**, pp. 595.
10. Sharma, Y.; Tiwari, A.; Hattori, S.; Terada, D.; Sharma, A.K.; Ramalingam, M.; Kobayashi, H.; *Int. J. Biol. Macromol.* **2012,** *51*, 627.
    DOI: 10.1016/j.ijbiomac.2012.06.014
11. Sharma, A.K.; Sharma, Y.; *Analytical Lett.* **2012,** *45,* 2075.
    DOI: 10.1080/00032719.2012.680057
12. Qian, D.; Dickey, E.C.; Andrews, R.; Rantell, T.; *Appl. Phys. Lett.* **2000**, *76*, 2868.
    DOI: 10.1063/1.126500
13. Kim, J.H.; Sharma, A.K.; Lee, Y.S.; *Mat. Lett.* **2006**, *60*, 1697.
    DOI: 10.1016/j.matlet.2005.12.002
14. Kargirwar, S.R.; Thakare, S.R.; Choudhary, M.D.; Kondawar, S.B.; Dhakate, S.R.; *Adv. Mat. Lett.* **2011**, *2*, 397.
    DOI: 10.5185/amlett.2011.4245
15. Kondawar, S.B.; Acharya, S.A.; Dhakate, S.R.; *Adv. Mat. Lett.* **2011**, *2*, 362.
    DOI: 10.5185/amlett.2011.9107am2011
16. Karim, M.R.; Lee, C.J.; Park, Y.T.; Lee, M.S.; *Synth. Met.* **2005**, *151*, 131.
    DOI: 10.1016/j.synthmet.2005.03.012
17. Kushwah, B.S.; Upadhyaya, S.C.; Shukla, S.; Sikarwar, A.S.; Sengar, R.M.S.; Bhaduria, S.; *Adv. Mat. Lett.* **2011**, *2*, 43.
    DOI: 10.5185/amlett.2010.8149
18. Guo, H.; Zhu, H.; Lin, H.; Zhang, J.; *Colloid Polym Sci.* **2008**, *286*, 587.
    DOI: 10.1007/s00396-007-1828-0
19. Kim, J.H.; Lee, Y.S.; Sharma, A.K.; Liu, C.G.; *Electrochimica Acta.* **2006**, *52*, 1727.
    DOI: 10.1016/j.electacta.2006.02.059
20. Zhou, Y.; Qin, Z.Y.; Li L., Zhang, Y.; Wei, Y.L.; Wang, L.F.; Zhu, M.F.; *Electrochim. Acta,* **2010**, *55*, 3904.
    DOI: 10.1016/j.electacta.2010.02.022
21. Iijima, Sumio, "Helical microtubules of graphitic carbon", *Nature* **1991**, *354*, 56.
    DOI: 10.1038/354056a0
22. Geim, A.K.; Novoselov, K.S.; The Rise of Graphene, *Nat. Mater.* **2006**, *6*, 183.
    DOI: 10.1038/nmat1849
23. Gustavo M.Do Nascimento, Spectroscopy of Polyaniline Nanofibers, **2010.**
    ISBN: 978-953-7619-86-2
24. Mavundla, Sipho E.; Malgas, Gerald F.; Motaung, David E.; Iwuoha Emmanuel I.; *J Mater Sci* **2010**, *45*, 3325.
    DOI: 10.1007/s10853-010-4351-5
25. Zhu,Y.F.; Zhang, L.; Natsuki,T.; Fu,Y.Q.; Qing-Qing Ni *Synthetic Metals* **2012**, *162*, 337.
    DOI: 10.1016/j.synthmet.2011.12.015
26. Xu, P.; Han, X.J.; Wang, C.; Zhang, B.; Wang, H.L.; *Synthetic Metals* **2009**, *159*, 430.
    DOI: 10.1016/j.synthmet.2008.10.016
27. Gupta, S.; *J. Raman Spectroscopy,* **2008,** *39*, 1343.
    DOI: 10.1002/jrs.2002
28. Demoustier-Champagne, S.; Stavaux, P.Y.; *Chem. Mat.*, **1999**, *11*, 829.
    DOI: 10.1021/cm9807541
29. Santos, M.J.L.; Brolo, A.G.; Girotto, E.M.; *Electrochimica Acta* **2007** *52*, 6141.
    DOI: 10.1016/j.electacta.2007.03.070
30. Mažeikienė, R.; Niaura, G.; Malinauskas, A.; *Polym. Degrad. Stab.* **2008**, *93*, 1742.
    DOI: 10.1016/j.polymdegradstab.2008.07.028
31. Mishra, A.K.; Ramprabhu, S.; *AIP Advances* **2012**, *2*, 022121
    DOI: 10.1063/1.4717490.
32. Cheng, Q.; Tang, J.; Shinya, N.; Qin, L.C.; *J. Power Sources* **2013**, *241*, 423.
    DOI: 10.1016/j.jpowsour.2013.04.105